

Neural network-based formula for shear capacity prediction of one-way slabs under concentrated loads

Abambres, Miguel; Lantsoght, Eva O.L.

DOI

[10.1016/j.engstruct.2020.110501](https://doi.org/10.1016/j.engstruct.2020.110501)

Publication date

2020

Document Version

Accepted author manuscript

Published in

Engineering Structures

Citation (APA)

Abambres, M., & Lantsoght, E. O. L. (2020). Neural network-based formula for shear capacity prediction of one-way slabs under concentrated loads. *Engineering Structures*, 211, Article 110501. <https://doi.org/10.1016/j.engstruct.2020.110501>

Important note

To cite this publication, please use the final published version (if applicable). Please check the document version above.

Copyright

Other than for strictly personal use, it is not permitted to download, forward or distribute the text or part of it, without the consent of the author(s) and/or copyright holder(s), unless the work is under an open content license such as Creative Commons.

Takedown policy

Please contact us and provide details if you believe this document breaches copyrights. We will remove access to the work immediately and investigate your claim.

Highlights

- This paper presents a database of 287 reinforced concrete slabs failing in shear.
- Artificial neural networks are used to find a matrix-based expression.
- The developed expression can be used for the assessment of slab bridges.
- As mechanical models are lacking, the presented expression can be used to predict the shear capacity of slabs.
- The matrix-based expression gives insight in the sensitivity to certain parameters.

1 **Neural network-based formula for shear capacity prediction of one-**
2 **way slabs under concentrated loads**

3 **Miguel ABAMBRES¹, Eva O.L. LANTSOGHT^{2,3*}**

4 ¹ R&D, Abambres' Lab, 1600-275 Lisbon, Portugal

5 ² Politécnico, Universidad San Francisco de Quito, Quito, Ecuador

6 ³ Concrete Structures, Department of Engineering Structures, Delft University of Technology,
7 Delft, the Netherlands

8 ***Corresponding Author**

9 E.O.L.Lantsoght@tudelft.nl

10 **Abstract**

11 According to the current codes and guidelines, shear assessment of existing reinforced concrete
12 slab bridges sometimes leads to the conclusion that the bridge under consideration has
13 insufficient shear capacity. The calculated shear capacity, however, does not consider the
14 transverse redistribution capacity of slabs, and thus leads to overly conservative values. While
15 mechanics-based models have attempted to describe the problem of one-way shear in concrete
16 slabs under concentrated loads, this problem is still not fully understood. Therefore, this paper
17 proposes an artificial neural network (ANN)-based formula to come up with estimates of the
18 shear capacity of one-way reinforced concrete slabs under a concentrated load that are as good as
19 possible based on 287 test results obtained from the literature. The methods used for this purpose

20 are: (i) the development of the database with experimental results from the literature, and (ii) the
21 development of the ANN-based matrix formulation. For the latter purpose, many thousands of
22 ANN models were generated, based on 475 distinct combinations of fifteen typical ANN
23 features. The proposed “optimal” model yields maximum and mean relative errors of 0.0% for
24 the 287 datapoints. Moreover, it was illustrated to clearly outperform (mean $V_{test} / V_{ANN} = 1.00$)
25 the Eurocode 2 provisions (mean $V_{E,EC} / V_{R,c} = 1.59$) for that dataset. A step-by-step assessment
26 scheme for reinforced concrete slab bridges by means of the ANN-based model is also proposed
27 in this work, which results in an improvement of the current assessment procedures.

28 **Keywords:** Artificial Neural Networks; Bridges; Design Formula; One-Way Slabs; Reinforced
29 Concrete; Shear Capacity

30

31 **1. Introduction**

32 As the age of existing infrastructures is increasing, the question if existing structures are safe for
33 further operation becomes important. To answer this question, an accurate assessment of the
34 existing infrastructures is necessary. The assessment should not be overly conservative, so that
35 unnecessary strengthening or replacement actions can be avoided. On the other hand, the
36 assessment should be as accurate as possible, so that structural safety can be assured.

37 When reinforced concrete slab bridges are assessed, the estimated one-way shear capacity can be
38 overly conservative, as transverse redistribution is not considered in the existing codes [1, 2]. In
39 Europe, the live load model from NEN-EN 1991-2:2003 [3] uses a distributed lane load and
40 design tandems. These tandems consist of large concentrated loads that are closely spaced, so that
41 the load combination with the currently prescribed load model in Europe leads to large shear
42 stresses at the support. As a result, a large number of reinforced concrete slab bridges are found
43 to be insufficient for shear when assessed according to the currently governing codes [4]. While
44 the shear provisions fulfil the purpose for design (i.e. ensuring that the designed bridge fails in
45 flexure before shear), it does not fulfil the purpose for assessment (i.e. separating the bridges that
46 pose a safety risk and require strengthening from those that are only shear-critical according to
47 the conservative code formulas but, when analyzed further, fulfil the safety requirements when
48 additional shear-carrying mechanisms are taken into account).

49 For more than a century [5-7], researchers have been debating the shear capacity of reinforced
50 concrete members without shear reinforcement [8-10]. In slabs, the additional dimension of the
51 width makes the problem three-dimensional [11, 12]. A plasticity-based model [13, 14] has been
52 proposed to estimate the maximum load on a reinforced concrete slab bridge, but this method has

53 the disadvantage that the calculation needs to be tailored to the geometry of the bridge under
54 consideration. Nonlinear finite element models [15] combined with the appropriate safety formats
55 [16-19] can be used for the assessment of existing reinforced concrete slab bridges, but this
56 approach is quite time-consuming [20].

57 When a large number of bridges need to be assessed, computationally fast methods are necessary.
58 To determine the sectional shear stresses and bending moments due to the applied load
59 combination, automated procedures using linear finite element models can be. Determining the
60 bending moment capacity can be based on the traditional flexural theory for reinforced concrete
61 beams. For a more effective estimate of the shear capacity of one-way reinforced concrete slabs
62 under a concentrated load, this paper proposes the use of artificial neural networks (ANN), a
63 popular machine learning technique. This approach results in an improvement of the estimation
64 of the shear capacity of reinforced concrete one-way slabs failing in shear. Moreover, the
65 proposed ANN-based model can be used for the assessment of one-way reinforced concrete slab
66 bridges. This paper contains a step-by-step approach for the assessment of such bridges.

67 Machine learning, one of the six disciplines of Artificial Intelligence (AI) without which the task
68 of having machines acting humanly could not be accomplished, allows us to ‘teach’ computers
69 how to perform tasks by providing examples of how they should be done [21]. When there is
70 abundant data (also called examples or patterns) explaining a certain phenomenon, but its theory
71 richness is poor, machine learning can be a perfect tool; as such its application to the problem of
72 shear in one-way slabs is suitable and timely. The Artificial Neural Network (also referred in this
73 manuscript as ANN or neural net) is the (i) oldest [22] and (ii) most powerful [23] technique of
74 machine learning. ANNs also lead the number of practical applications, virtually covering any
75 field of knowledge [24, 25]. In its most general form, an ANN is a mathematical model designed

76 to perform a particular task, based in the way the human brain processes information, i.e. with the
77 help of its processing units (the neurons). ANNs have been employed to perform several types of
78 real-world basic tasks, and have been successfully applied to civil engineering problems [26-41].
79 Some efforts have also been geared towards using ANN-based prediction models for the problem
80 related to shear in structural concrete, yet these models still have relatively large errors [42-49].
81 Concerning functional approximation, ANN-based solutions are frequently more accurate than
82 those provided by traditional approaches, such as multi-variate nonlinear regression, besides not
83 requiring a good knowledge of the function shape being modelled [50]. The proposed ANN was
84 designed based on the 287 experimental results available to date in the literature.

85 The goal of this study is not to provide a full description of the mechanics underlying the
86 behavior of one-way reinforced concrete slabs. While research efforts are being geared towards
87 understanding the mechanics behind the shear capacity of reinforced concrete slabs, the proposed
88 approach allows us to use the available experimental data in an optimal way, and to address the
89 current need for the assessment of reinforced concrete slab bridges with computationally efficient
90 tools.

91 **2. Research significance**

92 This work proposes a new way to determine the shear capacity of reinforced concrete one-way
93 slabs based on artificial neural networks. For this study, a unique database (available in the public
94 domain) of 287 experimental results is analyzed. The analysis is based on combining different
95 possible features of artificial neural networks, and finding the best performing matrix-based
96 expression. This new expression has a practical application as well: it can be used for the design

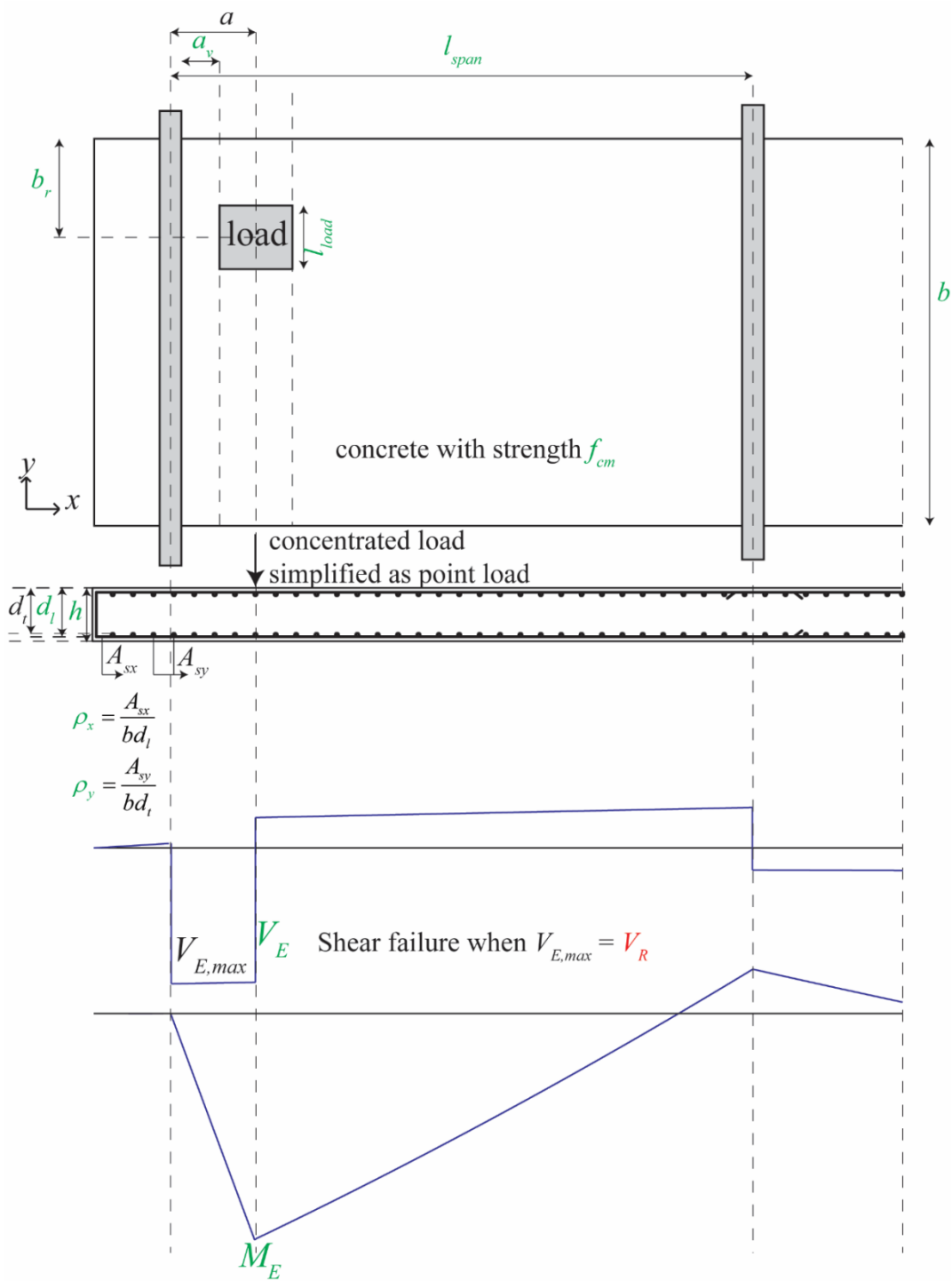
97 and analysis of reinforced concrete slab bridges, as suitable physical models for this problem are
98 currently not available.

99 **3. Data Gathering**

100 The dataset used for the development of the ANN simulations consists of 287 experimental
101 results from (i) tests gathered from the literature reported in [51], consisting of references [52-
102 85], (ii) the TU Delft slab shear tests [86], and (iii) recently reported experiments [87]. The
103 collected experiments are on slabs and wide beams, under line loads and concentrated loads. The
104 specimens are either cantilevers, simply supported slabs, continuously supported slabs, or
105 experiments carried out on slab bridges. Analyzing the test results shows that the minimum value
106 of $b/d_l = 0.57$, the maximum value is 46.30 and the average is 10.40, showing that the majority of
107 the experiments would classify as slabs according to the ratio $b/d_l \geq 5$. Additionally, we
108 considered that a certain amount of transverse load redistribution also occurs for wide beams
109 subjected to a load that does not act over its full width. Eleven variables were adopted as input
110 (independent) for the ANN-based shear capacity predictions, as described and illustrated in Table
111 1 and Fig. 1, respectively. Fig. 1 shows the resulting bending moment and shear diagrams when
112 the slab is considered as a beam model, the supports are considered as point supports, and the
113 load is considered as a point load.

114 Table 1 also gives the minimum and maximum value for each parameter in the database. As can
115 be seen in Table 1, the range of parameters covers the geometry of laboratory-sized specimens to
116 actual bridges tested to collapse in the field. The range of values for the concrete compressive
117 strength covers from low strength concrete to high strength, which is often found in existing
118 reinforced concrete slab bridges as the result of ongoing cement hydration. The reinforcement

119 ratios in the database also encompass the values encountered in existing slab bridges. The large
 120 range of parameters for the loading conditions aims to reflect the assessment practice, where the
 121 main contribution to the sectional shear comes from the design tandem.



122

123 **Fig. 1. Input (independent) and output (dependent) variables considered in ANN design.**

124 Note that the proposed ANN features just 10 nodes in the first layer, which inputs have to be
 125 obtained as function of those eleven variables, as described in §3.7.1. For all experiments, the
 126 sectional shear and moment were calculated considering all loads, thus including the self-weight.
 127 For the case of a continuous slab shown in Fig. 1, the slight gradient in the shear diagram and the
 128 slight nonlinearity in the bending moment diagram are caused by the self-weight. All values of
 129 the concrete compressive strength are the cylinder compressive strength. This value was either
 130 reported in the original reference, or calculated as 82% of the cube compressive strength [88].
 131 The corresponding 287-point dataset is publicly available [89], and was constructed by randomly
 132 ordering the collected experimental results.

133 **Table 1. Variables adopted in the study, showing minimum and maximum values in the**
 134 **database.**

Input Variables			min	max	Input
Slab geometry	b (m)	slab width	0.249	11.125	1
	h (m)	slab height	0.100	1.005	2
	d_l (m)	slab effective depth	0.080	0.916	6
	l_{span} (m)	span length	0.600	12.192	9
Material	f_{cm} (MPa)	average concrete cylinder compressive strength	12.4	77.7	3
Reinforcement	ρ_x (-)	longitudinal reinforcement ratio	0.003	0.028	4
	ρ_y (-)	transverse reinforcement ratio	0	0.015	5
Loading parameters	b_r (m)	distance from slab edge to the center of the load	0.125	5.563	7
	l_{load} (m)	dimension of the loading plate (wheel print)	0.070	2.519	8
	$M_E/V_E d_l$ (-)	ratio of sectional moment to product of sectional shear and effective depth	0.14	10.75	10
	a_v/d_l (-)	ratio of clear shear span to effective depth	0.00	6.88	11

Output Variables				Output
V_R (kN)	shear capacity	35	2444	1

135

136

137 **4. Artificial Neural Networks**

138 **4.1 General approach**

139 The general ANN structure consists of several nodes in L vertical interconnected layers (input
140 layer, hidden layers, and output layer). Between each node (or neuron) in layers 2 to L is a linear
141 or nonlinear transfer function. All ANNs implemented in this work are feedforward. The neural
142 network is developed through “learning”: determining the synaptic weight of the connection
143 between two nodes, and each neuron’s bias. To find the optimal matrix-based expression for the
144 problem under study, 15 ANN features were varied in this work. Tables 2-4 show the 15 ANN
145 features that were varied in this study. The code was developed in MATLAB [90] with its neural
146 network toolbox for using popular learning algorithms (1-3 from F13 in Table 4). Each
147 parametric sub-analysis (SA) consists of running all feasible combinations of pre-selected
148 methods for each ANN feature and finding the associated performance results for each designed
149 net. This approach then allows selection of the “best” neural net for the problem under study. The
150 best network is the one exhibiting the smallest average relative error for all learning data. The
151 developed algorithm is validated [91]. The interested reader can find more background on the
152 development of the algorithm to find the optimal neural network in [92].

153 **Table 2. Implemented ANN features (F) 1-5.**

FEATURE	F1	F2	F3	F4	F5
METHOD	Qualitative Var Represent	Dimensional Analysis	Input Dimensionality Reduction	% Train-Valid- Test	Input Normalization
1	Boolean Vectors	Yes	Linear Correlation	80-10-10	Linear Max Abs
2	Eq Spaced in]0,1]	No	Auto-Encoder	70-15-15	Linear [0, 1]
3	-	-	-	60-20-20	Linear [-1, 1]
4	-	-	Ortho Rand Proj	50-25-25	Nonlinear
5	-	-	Sparse Rand Proj	-	Lin Mean Std
6	-	-	No	-	No

154 **Table 3. Implemented ANN features (F) 6-10.**

FEATURE	F6	F7	F8	F9	F10
METHOD	Output Transfer	Output Normalization	Net Architecture	Hidden Layers	Connectivity
1	Logistic	Lin [a, b] = $0.7[\varphi_{\min}, \varphi_{\max}]$	MLPN	1 HL	Adjacent Layers
2	-	Lin [a, b] = $0.6[\varphi_{\min}, \varphi_{\max}]$	RBFN	2 HL	Adj Layers + In-Out
3	Hyperbolic Tang	Lin [a, b] = $0.5[\varphi_{\min}, \varphi_{\max}]$	-	3 HL	Fully-Connected
4	-	Linear Mean Std	-	-	-
5	Bilinear	No	-	-	-
6	Compet	-	-	-	-
7	Identity	-	-	-	-

155 Abbreviations: MLPN = multi-layer perceptron net, RBFN = radial basis function net

156 **Table 4. Implemented ANN features (F) 11-15.**

FEATURE	F11	F12	F13	F14	F15
METHOD	Hidden Transfer	Parameter Initialization	Learning Algorithm	Performance Improvement	Training Mode

1	Logistic	Midpoint (W) + Rands (b)	BP	NNC	Batch
2	Identity-Logistic	Rands	BPA	-	Mini-Batch
3	Hyperbolic Tang	Randnc (W) + Rands (b)	LM	-	Online
4	Bipolar	Randnr (W) + Rands (b)	ELM	-	-
5	Bilinear	Randsmall	mb ELM	-	-
6	Positive Sat Linear	Rand [- Δ , Δ]	I-ELM	-	-
7	Sinusoid	SVD	CI-ELM	-	-
8	Thin-Plate Spline	MB SVD	-	-	-
9	Gaussian	-	-	-	-
10	Multiquadratic	-	-	-	-
11	Radbas	-	-	-	-

157 Abbreviations: SVD = singular value decomposition, MB SVD = mini batch SVD, BP = back
158 propagation, BPA = back propagation with adaptive learning rate, LM = Levenberg-Marquardt,
159 ELM = extreme learning machine, mb-ELM = mini batch ELM, I-ELM = incremental ELM, CI-
160 ELM = convex incremental ELM, NNC = neural network composite.

161 4.2 Development of matrix-based expression for shear capacity of one-way slabs

162 To reduce the computational time by reducing the number of combos to be analyzed, the
163 parametric simulation was divided into nine parametric SAs, where in each one, F7 takes a single
164 value, see Table 5 (the numbers represent the method number as in Tables 2-4). Summing up the
165 ANN feature combinations for all parametric SAs, a total of 475 combos were ran for this work.
166 Table 6 shows the corresponding relevant results in terms of error, performance, and
167 computational time. All results shown in Table 6 are based on target and output datasets
168 computed in their original format, i.e. free of any transformations due to output normalization
169 and/or dimensional analysis.

170 **Table 5. ANN feature (F) methods used in the best combo from each parametric sub-**
 171 **analysis (SA).**

SA	F1	F2	F3	F4	F5	F6	F7	F8	F9	F10	F11	F12	F13	F14	F15
1	1	2	6	2	5	1	1	1	1	1	3	2	3	1	3
2	1	2	6	2	1	7	1	1	1	1	3	2	5	1	3
3	1	2	1	3	5	1	1	1	1	1	3	2	3	1	3
4	1	2	1	3	5	1	2	1	1	1	3	2	3	1	3
5	1	2	1	4	5	1	3	1	1	1	3	2	3	1	3
6	1	2	1	4	5	7	4	1	1	1	3	2	3	1	3
7	1	2	1	1	5	7	5	1	1	1	3	2	3	1	3
8	1	2	1	1	5	7	5	1	1	1	5	5	3	1	3
9	1	2	1	1	5	7	5	1	2	3	5	5	3	1	3

172 **Table 6. Performance results for the best design from each parametric sub-analysis: (a)**
 173 **ANN, (b) NNC.**

SA	ANN				
	Max Error (%)	Performance		Total Hidden Nodes	Running Time / Data Point (s)
		All Data (%)	Errors > 3% (%)		
1	0.0	0.0	0.0	44	2.13E-04
2	559.9	34.0	88.2	70	1.46E-04
3	0.0	0.0	0.0	37	2.43E-04
4	0.0	0.0	0.0	37	3.38E-04
5	0.0	0.0	0.0	37	1.77E-04
6	0.0	0.0	0.0	40	2.22E-04
7	171.0	5.8	30.3	29	1.48E-04
8	55.0	4.8	48.8	37	2.27E-04
9	66.7	6.5	62.0	30	1.59E-04

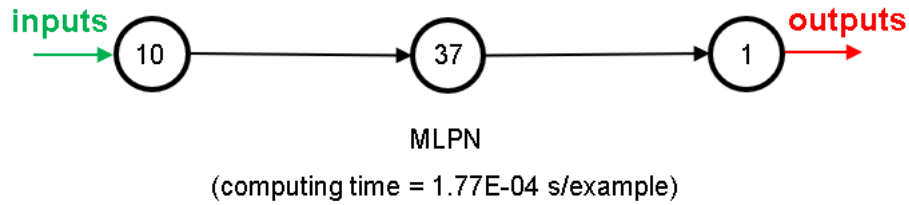
(a)

SA	NNC
----	-----

	Performance			Total Hidden Nodes	Running Time / Data Point (s)
	Max Error (%)	All Data (%)	Errors > 3% (%)		
1	-	-	-	-	-
2	-	-	-	-	-
3	-	-	-	-	-
4	-	-	-	-	-
5	-	-	-	-	-
6	-	-	-	-	-
7	9.2	0.3	4.5	29	1.79E-04
8	54.3	4.8	48.4	37	2.40E-04
9	49.7	5.2	53.0	30	1.67E-04

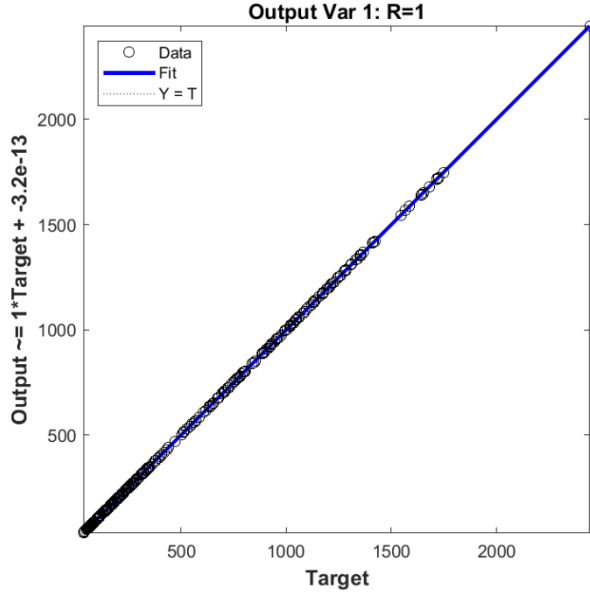
(b)

174 Several SAs yielded approximately null errors, see Table 6. Therefore, the ANN having the least
175 number of hidden nodes and the lowest running time per data point (SA 5) was selected as the
176 optimal model. This model is developed with 50% of the data used for training, 25% for
177 validation, and 25% for testing. To allow implementation of this model by any user, all
178 variables/equations required for (i) data preprocessing, (ii) ANN simulation, and (iii) data post-
179 processing, are available in the public domain [93]. The W and b arrays of the neural network are
180 available as a spreadsheet in the public domain, allowing direct implementation of the proposed
181 matrix-based formula [94]. The proposed model is a single MLPN with 3 layers and a
182 distribution of nodes/layer of 10-37-1. The network is partially-connected, and the hidden and
183 output transfer functions are all Hyperbolic Tangent and Logistic, respectively. The network was
184 trained using the Levenberg-Marquardt algorithm (2565 epochs). The analysis showed that the
185 column with d as input could be removed, resulting in 10 inputs. Fig. 2 depicts a simplified
186 scheme of some of the network key features. The obtained ANN solution for every data point can
187 be found in [89].



189 **Fig. 2 Proposed 10-37-1 partially-connected MLPN – simplified scheme.**

190 Finally, the results of the proposed ANN for the 287 datapoints, in terms of performance
191 variables are presented as: (i) a regression plot (Fig. 3), where network target and output data are
192 plotted, for each data point, as x - and y - coordinates respectively – a measure of linear correlation
193 is given by the Pearson Correlation Coefficient (R); (ii) a performance plot, where performance
194 (average error) values are displayed for several learning datasets, all of which give an error of
195 0%; and (iii) an error plot, where values concern all data (iii₁) maximum error and (iii₂) % of
196 errors greater than 3% (both cases give 0%). All graphical results just mentioned are based on
197 effective target and output values, i.e. computed in their original format (free of any
198 transformations due to output normalization).



199

200 **Fig. 3. Regression plot for the proposed ANN.**

201 **5. Sensitivity analysis**

202 As suggested by [38], a sensitivity analysis can be carried out with the following expression,

203 which determines the percentage effect of the i^{th} input variable on the output variable:

204

$$Q_i = \frac{\sum_{j=1}^{n_{\text{hidden}}} \frac{w_{ji}}{\sum_{l=1}^{n_{\text{inputs}}} |w_{jl}|} \times w_{oj}}{\sum_{i=1}^{n_{\text{inputs}}} \left(\sum_{j=1}^{n_{\text{hidden}}} \frac{w_{ji}}{\sum_{l=1}^{n_{\text{inputs}}} |w_{jl}|} \times w_{oj} \right)} \quad (1)$$

205 The sum of the connection weights between the 10 input neurons and the 37 hidden neurons is:

206

$$\sum_{l=1}^{n_{\text{inputs}}} |w_{jl}|$$

207 with w_{jl} the connection weight between the input neuron l and the hidden neuron j , and w_{oj} is the
 208 connection weight between the hidden neuron j and the output o .

209 Table 7 shows the results of this sensitivity analysis. The most important parameters are the total
 210 width b and the expression of the shear span to depth ratio based on the bending moment and
 211 shear diagram $M_E/V_E d_l$. The third most important factor is the concrete compressive strength f_{cm} ,
 212 which traditionally is considered as one of the most determining factors for the shear capacity. Of
 213 much less importance are the position of the load with respect to the width b_r and the total span
 214 length l_{span} .

215 **Table 7. Sensitivity analysis with Q_i the sensitivity of the i th input value.**

Input	Q_i (%)
b	47.05
h	7.01
f_{cm}	9.24
ρ_x	1.23
ρ_y	2.40
b_r	0.12
l_{load}	4.77
l_{span}	0.51
$M_E/V_E d_l$	20.38
a_v/d_l	7.29

216 6. ANN-based vs. Existing Models

217 Since the focus of this study is the assessment of reinforced concrete slab bridges in Europe, this
 218 section demonstrates the improved prediction capability of the ANN-based analytical model
 219 proposed in section 4, as compared to the shear capacity of one-way slabs predicted by the
 220 provisions of Eurocode 2 (NEN-EN 1992-1-1:2005 [95]). The reduction of the contribution of
 221 loads close to the support ($a_v \leq 2d_l$, see Fig. 1) to the sectional shear force prescribed by the
 222 Eurocode is taken into account, resulting in $V_{E,EC}$. This reduction corresponds to an increase in

223 the shear capacity for loads close to the support as a result of direct load transfer. Since this
 224 mechanism only occurs for loads applied on top of the cross-section and close to the support, the
 225 Eurocode 2 reduces the contribution of externally applied loads close to the support. As such, this
 226 provision allows for finding the sectional shear force for a combination of loads – a situation that
 227 occurs when assessing existing reinforced concrete slab bridges. The corresponding average
 228 shear capacity according to Eurocode 2 is determined as:

$$V_{R,c} = 0.15k(100\rho_x f_{cm})^{1/3} b_{eff} d_l \geq 0.035k^{3/2} \sqrt{f_{cm}} b_{eff} d_l \quad , (2)$$

$$k = 1 + \sqrt{\frac{200mm}{d_l}} \leq 2$$

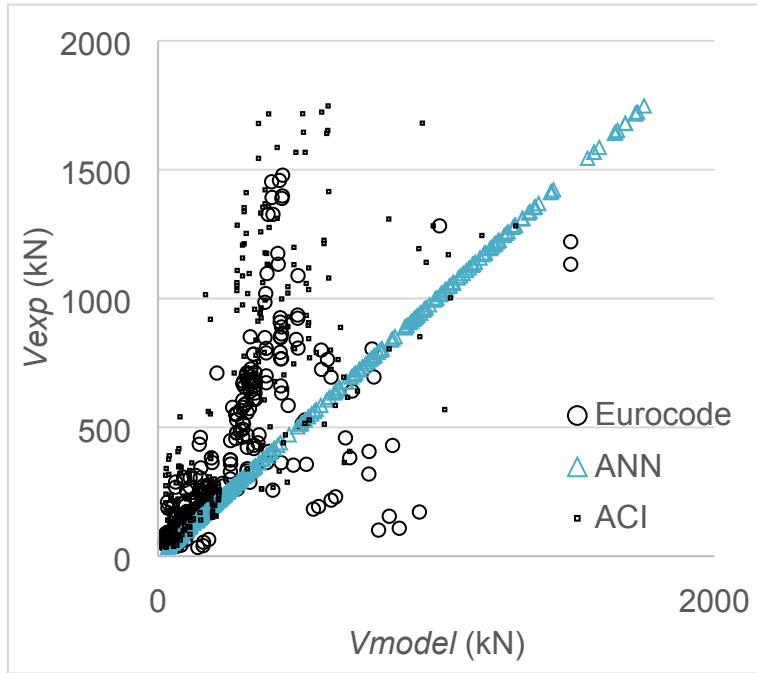
232
 233
 234 with (i) k the size effect factor, (ii) ρ_x the longitudinal reinforcement ratio, (iii) f_{cm} the average
 235 concrete cylinder compressive strength in [MPa], (iv) b_{eff} the effective width for one-way shear,
 236 determined with a 45° horizontal load spreading from the loading plate back edge to the face of
 237 the support, and (v) d_l the effective depth to the longitudinal reinforcement. $C_{R,c} = 0.15$ is used to
 238 find average values [96].

239 In addition to the Eurocode provisions, the shear provisions from ACI 318-14 [97] are also
 240 analyzed. The reader should note that these provisions are for building slabs, and thus not directly
 241 applicable to slab bridges. The design shear capacity according to ACI 318-14 equals:

$$V_{ACI,d} = 0.167\sqrt{f_c'} b_w d \quad (3)$$

243 with f_c' the specified concrete compressive strength in [MPa], b_w the web width, and d the
 244 effective depth. For application to slabs and for finding the average shear capacity $V_{ACI,m}$, f_c' is
 245 replaced with f_{cm} , b_w with b_{eff} , and d with d_l .

246



247

248 **Fig. 4. Comparison between tested and predicted shear capacities: Eurocode 2 and ACI**

249 **318-14 vs. proposed ANN.**

250 The average value of the ratio $V_{E,EC} / V_{R,c}$ (with $V_{E,EC}$ the sectional shear force taking into account
251 the reduction of the contribution of loads close to the support, and $V_{R,c}$ according to Eq. 2) for the
252 287 experimental results is 1.59, with a standard deviation of 0.79 and a coefficient of variation
253 of 49%. The reduction for loads close to the support applies to 151 datapoints of the database.

254 The average value of the ratio $V_{test} / V_{ACI,m}$ for the 287 experimental results is 2.36, with a standard
255 deviation of 1.74 and a coefficient of variation of 74%. The poor performance of the ACI code is
256 explained by the fact that direct load transfer is not taken into account. This observation was
257 already made before [86]. For comparison, the average value of V_{test} / V_{ANN} (with V_{test} the
258 sectional shear force at failure in each experiment, and V_{ANN} the ANN-based shear capacity) is
259 1.00, with a standard deviation of 5×10^{-14} and a coefficient of variation of 0.0%. The major
260 improvement of the ANN as compared to the Eurocode and ACI code is also shown in Fig. 4,

261 where the x -axis shows the predicted shear capacity V_{model} (V_{ANN} or $V_{R,c}$) and the y -axis shows the
262 experimental result V_{exp} , which is $V_{E,EC}$ for comparison to the Eurocode shear capacity and V_{test}
263 for comparison to the ANN-predicted shear capacity and ACI code. Fig. 4 shows the results for
264 the 287 datapoints used in this study.

265 7. Discussion

266 The results in Fig. 4 show the major improvement, for the 287-point dataset used, of the proposed
267 ANN-based model as compared to currently used Eurocode 2 and ACI 318 expressions for the
268 shear capacity of reinforced concrete slabs in one-way shear. One critical observation should be
269 made here: the ANN predictions are only valid within the input variable ranges of the employed
270 287-point dataset [89]. The number of experiments is rather limited, since slab shear tests are
271 expensive to carry out. The user should keep this restriction in mind when predicting the shear
272 capacity with the proposed ANN. The dataset covers a large number of variables that influence
273 the shear assessment of reinforced concrete, but all tested slabs are rectangular. For skewed slabs,
274 shear stress concentrations will result in the obtuse angle [98-100], making the skew angle an
275 important factor for the shear assessment. Besides the Liverpool experiments on skewed slabs
276 [101], which did not result in shear failures of the slabs, the authors are not aware of experiments
277 on skewed slabs under concentrated loads failing in one-way shear. To extend this novel ANN-
278 based design approach to new scenarios, experiments on skewed slabs failing in one-way shear
279 should be carried out, and the skew angle should then be included as input variable for ANN
280 design.

281 From Fig. 4, we can observe that there are 56 experiments for which Eurocode 2 EN 1992-1-
282 1:2005 leads to unsafe predictions. There are three reasons for this observation. The first reason is

283 related to the way in which concentrated loads on slabs are considered. For the calculations
284 shown in this work, a 45-degree load spreading between the far side of the loading plate and the
285 face of the support is used. We can observe that this approach seems not to perform equally well
286 for loads close to the support as for loads further away from the support. The second reason is
287 that the database contains slabs and wide beams in different loading schemes. Analyzing the
288 results shows that the Eurocode-based approach tends to be unconservative for cantilever slabs,
289 yet perform well for simply supported or continuously supported slabs. The third reason is that
290 the sectional shear in this analysis is calculated based on the sectional shear caused by self-weight
291 and the sectional shear caused by the load applied in the experiment, based on the principle of
292 superposition. Analysis of the results show that large members, where the self-weight is
293 considerable, lead to unsafe predictions. These observations should be considered in the next
294 round of revisions of EN 1992-1-1:2005, and should lie at the basis of better methods for taking
295 into account the contribution of concentrated loads in slabs.

296 To use the developed ANN formulation for the assessment of existing reinforced concrete one-
297 way slab bridges, the following procedure is proposed:

- 298 1. Make a linear finite element model (LFEM) of the bridge under consideration.
- 299 2. Apply the superimposed dead load and live load model on the LFEM.
- 300 3. Make the factored load combination according to the governing code.
- 301 4. Find the governing sectional shear force v_u based on a distribution of the peak shear stress
302 over $4d_l$ [102] and find the governing sectional moment m_E (including the effect of the
303 twisting moments [103]) based on a distribution of the peak sectional moment over $2d_l$.

- 304 5. Determine the shear capacity with the proposed ANN (V_{ANN}), taking as input the
305 characteristic material properties (where possible updated with measured values) and the
306 value of $M_E/(V_E d_l)$ where this ratio is maximum. Divide V_{ANN} by $4d_l$ to find v_{ANN} .
- 307 6. Determine the bending moment capacity m_R based on the flexural theory of concrete
308 elements.
- 309 7. Determine the Unity Check for shear: $UC_v = v_u/v_{ANN}$. If $UC_v \leq 1$, the requirements for
310 shear are fulfilled.
- 311 8. Determine the Unity Check for bending moment: $UC_m = m_E/m_R$. If $UC_m \leq 1$, the
312 requirements for bending moment are fulfilled.
- 313 9. If $UC_v > UC_m$ the bridge can be considered as shear-critical: shear failure is expected to
314 occur before flexural failure.

315 When either UC_v or UC_m is found to be larger than 1, more refined methods, such as nonlinear
316 finite element analysis or proof load testing, may be necessary for a sharper assessment of the
317 bridge under consideration. The proposed method is fast, cheap, and computationally efficient,
318 and as such it is especially suitable for cases where a large number of bridges need to be assessed.

319 The sensitivity analysis gives us a unique insight in the most important parameters for the shear
320 capacity of reinforced concrete slabs failing in one-way shear. Based on these results, we find
321 that the ratio $M_E/V_E d_l$ and the overall width b are the parameters that have the largest impact on
322 the resulting shear capacity. In general, we can observe in Table 7 that the parameters related to
323 the geometry of the load and the slab govern the shear behavior. This observation confirms the
324 hypothesis from [86], which was one of the starting points for the lower-bound plasticity-based
325 analysis method for one-way slabs failing in shear, the Extended Strip Model [13, 14].

326 The proposed approach is a tool to use the available experimental data to address a practical
327 problem where mechanical models have not been able to yield good predictions yet. While it is of
328 the utmost importance to develop better mechanical models so that we can understand the shear
329 failure of reinforced concrete slabs, such a development may still require some time. Therefore,
330 we propose our developed matrix-based formula to address the current need to estimate more
331 accurately the shear capacity of reinforced concrete slab bridges.

332 The main novelty of this work is that the available experimental results are analyzed and that an
333 accurate model is presented. Not only can this model be used to predict shear capacities in
334 experiments; the range of parameters covers the range of practical values for short span
335 reinforced concrete slab bridges. As such, the proposed model has a direct practical implication.
336 To the authors' knowledge, no other ANN-based expression is available for estimating the shear
337 capacity of reinforced concrete one-way slabs. From this point of view, the proposed method is
338 the first in its kind. As compared to other ANN-based expressions for structural concrete
339 applications, the large number of ANN features that we explored in this study are an
340 improvement as compared to the applications we encountered in the literature, which are based
341 on the features provided in the standard ANN toolbox of Matlab. The result of this approach is
342 that our proposed ANN-based expression has lower errors than those reported for other ANN-
343 based expressions for problems related to shear in structural concrete.

344 **8. Summary and conclusions**

345 This paper shows how artificial neural networks can be used to predict the shear capacity of one-
346 way slabs under concentrated loads.

- 347 • For this purpose, a database with 287 experimental results was compiled. From this
348 dataset, 10 governing parameters were identified as input variables and the sectional shear
349 force at failure was considered the output variable.
- 350 • The proposed ANN-based analytical model (with 50% of the data used for training, 25%
351 for validation and 25% for testing) yielded maximum and mean relative errors of 0.0%
352 and 0.0% for those 287 points, respectively. Moreover, it was illustrated to clearly
353 outperform (mean $V_{test}/V_{ANN}=1.00$) the Eurocode 2 provisions (mean $V_{E,EC}/V_{R,c}=1.59$)
354 and the ACI 318-14 provisions (mean $V_{test}/V_{ACI}=2.36$) for that dataset.
- 355 • A sensitivity analysis of the ANN-based model showed that the most important input
356 parameters are the width of the slab, the effect of the shear span to depth ratio represented
357 by the ratio of the sectional moment to the product of the sectional shear and effective
358 depth, and the concrete compressive strength.
- 359 • Lastly, a step-by-step methodology for the assessment of existing reinforced concrete
360 one-way slab bridges, based on the use of the developed ANN-based formula, was
361 proposed.

362 The study carried out has not yet allowed a full description of the mechanics underlying the
363 behavior of one-way reinforced concrete slabs, but parametric studies by means of ANN-based
364 models make it possible to evaluate and improve existing mechanical models.

365 **Notations**

- 366 a center-to-center distance between load and support
367 a_v face-to-face distance between load and support
368 b width

369	b_{eff}	effective width for concentrated loads on slabs
370	b_r	distance from edge to load in the transverse direction
371	b_w	web width
372	d	effective depth
373	d_l	effective depth to the longitudinal reinforcement
374	d_t	effective depth to transverse reinforcement
375	f_c'	specified concrete compressive strength
376	f_{cm}	average concrete cylinder compressive strength
377	h	height of cross-section
378	k	size effect factor
379	l_{load}	size of the loading plate, in the y -direction
380	l_{span}	span length
381	m_E	moment in slab
382	m_R	moment resistance
383	v_{ANN}	shear capacity (stress) derived from V_{ANN}
384	v_u	shear in slab
385	w_{ji}	connection weight between the neuron i and the neuron j
386	w_{jl}	connection weight between the input neuron l and the hidden neuron j
387	w_{oj}	connection weight between the hidden neuron j and the output o
388	A_{sx}	area of steel in the longitudinal direction
389	A_{sy}	area of steel in the transverse direction
390	M_E	sectional moment caused by self-weight and loads applied during experiment
391	R	pearson correlation coefficient
392	Q_i	sensitivity of i -th parameter

- 393 UC_m unity check for bending moment
- 394 UC_v unity check for shear
- 395 $V_{ACI,d}$ design capacity according to ACI 318-14
- 396 $V_{ACI,m}$ average capacity based on design capacity from ACI 318-14
- 397 V_{ANN} shear capacity determined with ANN-based model
- 398 V_{exp} experimental shear capacity
- 399 V_E sectional shear caused by self-weight and loads applied during experiment
- 400 $V_{E,EC}$ governing sectional shear, keeping into consideration the reduction of loads close to the
- 401 support prescribed in EN 1992-1-1:2005
- 402 $V_{E,max}$ sectional shear at governing cross-section, maximum absolute value of V_E
- 403 V_{model} shear capacity predicted with model
- 404 V_R shear resistance
- 405 $V_{R,c}$ mean shear resistance calculated with EN 1992-1-1:2005
- 406 V_{test} sectional shear force at failure in experiments
- 407 ρ_x amount of reinforcement in the longitudinal direction
- 408 ρ_y amount of reinforcement in the transverse direction

409 **References**

- 410
- 411 [1] Lantsoght EOL, van der Veen C, de Boer A, Walraven JC. Recommendations for the Shear
- 412 Assessment of Reinforced Concrete Slab Bridges from Experiments Structural Engineering
- 413 International. 2013;23:418-26.

- 414 [2] Lantsoght EOL, van der Veen C, de Boer A, Walraven J. Transverse Load Redistribution and
415 Effective Shear Width in Reinforced Concrete Slabs. *Heron*. 2015;60:145-80.
- 416 [3] CEN. Eurocode 1: Actions on structures - Part 2: Traffic loads on bridges, NEN-EN 1991-
417 2:2003. Brussels, Belgium: Comité Européen de Normalisation; 2003. p. 168.
- 418 [4] Walraven JC. Residual shear bearing capacity of existing bridges. *fib Bulletin 57, Shear and*
419 *punching shear in RC and FRC elements; Proceedings of a workshop held on 15-16 October*
420 *2010. Salò, Lake Garda, Italy 2010. p. 129-38.*
- 421 [5] Talbot AN. Tests of reinforced concrete T-beams. Urbana: University of Illinois; 1906. p. 42.
- 422 [6] Talbot AN. A test of three large reinforced concrete beams. Urbana: University of Illinois;
423 1908. p. 42.
- 424 [7] Talbot AN. Tests of reinforced concrete beams. Urbana: University of Illinois; 1905. p. 92.
- 425 [8] Kani GNJ. The Riddle of Shear Failure and Its Solution. *ACI Journal Proceedings*.
426 1964;61:441-67.
- 427 [9] Collins MP, Kuchma D. How safe are our large, lightly reinforced concrete beams, slabs, and
428 footings? *ACI Structural Journal*. 1999;96:482-90.
- 429 [10] Regan PE. Research on shear: a benefit to humanity or a waste of time. *The structural*
430 *engineer*. 1993;71:337-47.
- 431 [11] Lantsoght EOL, van der Veen C, Walraven JC. Shear in One-way Slabs under a
432 Concentrated Load close to the support. *ACI Structural Journal*. 2013;110:275-84.

- 433 [12] Lantsoght EOL, Van der Veen C, Walraven JC, De Boer A. Transition from one-way to
434 two-way shear in slabs under concentrated loads. Magazine of Concrete Research. 2015;67:909-
435 22.
- 436 [13] Lantsoght EOL, van der Veen C, de Boer A. Extended Strip Model for slabs subjected to
437 load combinations. Engineering Structures. 2017;145:60-9.
- 438 [14] Lantsoght EOL, van der Veen C, de Boer A, Alexander SDB. Extended Strip Model for
439 Slabs under Concentrated Loads. ACI Structural Journal. 2017;114:565-74.
- 440 [15] Falbr J. Shear redistribution in solid concrete slabs. Delft: Delft University of Technology;
441 2011.
- 442 [16] Belletti B, Damoni c, Hendriks MAN, Den Uijl JA. Nonlinear finite element analyses of
443 reinforced concrete slabs: comparison of safety formats. In: Van Mier JGM, Ruiz G, Andrade C,
444 Yu RC, Zhang XX, editors. VIII International Conference on Fracture Mecahnics of concrete and
445 Concrete Structures, FraMCoS-82013. p. 12.
- 446 [17] Blomfors M, Engen M, Plos M. Evaluation of safety formats for non-linear finite element
447 analyses of statically indeterminate concrete structures subjected to different load paths.
448 Structural Concrete. 2016;17:44-51.
- 449 [18] Schlune H. Safety Evaluation of Concrete Structures with Nonlinear Analysis. Gothenburg,
450 Sweden: Chalmers University; 2011.
- 451 [19] Schlune H, Plos M, Gylltoft K. Safety formats for nonlinear analysis tested on concrete
452 beams subjected to shear forces and bending moments. Engineering Structures. 2011;33:2350-6.

- 453 [20] Shu J, Bagge N, Plos M, Johansson M, Yang Y, Zandi K. Shear Capacity of a RC Bridge
454 Deck Slab: Comparison between Multilevel Assessment and Field Test. Journal of Structural
455 Engineering. 2018;144:04018081.
- 456 [21] Hertzmann A, Fleet D. Machine Learning and Data Mining, Lecture Notes CSC 411/D11.
457 Canada: Computer Science Department, University of Toronto; 2012.
- 458 [22] McCulloch WS, Pitts W. A logical calculus of the ideas immanent in nervous activity. The
459 bulletin of mathematical biophysics. 1943;5:115-33.
- 460 [23] Hern A. Google says machine learning is the future. So I tried it myself. 2016.
- 461 [24] Wilamowski BM, Irwin JD. The industrial electronics handbook. 2nd ed. Boca Raton, FL:
462 CRC ; Taylor & Francis distributor; 2011.
- 463 [25] Prieto A, Prieto B, Ortigosa EM, Ros E, Pelayo F, Ortega J et al. Neural networks: An
464 overview of early research, current frameworks and new challenges. Neurocomputing.
465 2016;214:242-68.
- 466 [26] Venkata Rao K, Murthy PBGSN. Modeling and optimization of tool vibration and surface
467 roughness in boring of steel using RSM, ANN and SVM. Journal of Intelligent Manufacturing.
468 2018;29:1533-43.
- 469 [27] Naser MZ. Deriving temperature-dependent material models for structural steel through
470 artificial intelligence. Construction and Building Materials. 2018;191:56-68.

471 [28] Yaseen ZM, Deo RC, Hilal A, Abd AM, Bueno LC, Salcedo-Sanz S et al. Predicting
472 compressive strength of lightweight foamed concrete using extreme learning machine model.
473 Advances in Engineering Software. 2018;115:112-25.

474 [29] Flood I, Kartam N. Neural Networks in Civil Engineering. I: Principles and Understanding. J
475 Comput Civil Eng. 1994;8:131-48.

476 [30] Mukherjee A, Deshpande JM, Anmala J. Prediction of Buckling Load of Columns Using
477 Artificial Neural Networks. Journal of Structural Engineering. 1996;122:1385-7.

478 [31] Aymerich F, Serra M. Prediction of fatigue strength of composite laminates by means of
479 neural networks. Key Engineering Materials. 1998;144:231-40.

480 [32] Pu Y, Mesbahi E. Application of artificial neural networks to evaluation of ultimate strength
481 of steel panels. Engineering Structures. 2006;28:1190-6.

482 [33] Gholizadeh S, Pirmoz A, Attarnejad R. Assessment of load carrying capacity of castellated
483 steel beams by neural networks. Journal of Constructional Steel Research. 2011;67:770-9.

484 [34] Weinstein Jordan C, Sanayei M, Brenner Brian R. Bridge Damage Identification Using
485 Artificial Neural Networks. Journal of Bridge Engineering. 2018;23:04018084.

486 [35] Naderpour H, Kheyroddin A, Amiri GG. Prediction of FRP-confined compressive strength
487 of concrete using artificial neural networks. Composite Structures. 2010;92:2817-29.

488 [36] Naderpour H, Mirrashid M. Shear Failure Capacity Prediction of Concrete Beam-Column
489 Joints in Terms of ANFIS and GMDH. Practice Periodical on Structural Design and
490 Construction. 2019;24:04019006.

- 491 [37] Naderpour H, Mirrashid M. An innovative approach for compressive strength estimation of
492 mortars having calcium inosilicate minerals. *Journal of Building Engineering*. 2018;19:205-15.
- 493 [38] Naderpour H, Nagai K, Fakharian P, Haji M. Innovative models for prediction of
494 compressive strength of FRP-confined circular reinforced concrete columns using soft computing
495 methods. *Composite Structures*. 2019;215:69-84.
- 496 [39] Naderpour H, Rafiean AH, Fakharian P. Compressive strength prediction of environmentally
497 friendly concrete using artificial neural networks. *Journal of Building Engineering*. 2018;16:213-
498 9.
- 499 [40] Abambres M, Lantsoght EOL. ANN-Based Shear Capacity of Steel Fiber-Reinforced
500 Concrete Beams without Stirrups. *Fibers*. 2019;7:88.
- 501 [41] Abambres M, Lantsoght EOL. ANN-Based Fatigue Strength of Concrete under
502 Compression. *Materials*. 2019;12:3787.
- 503 [42] Adhikary BB, Mutsuyoshi H. Prediction of shear strength of steel fiber RC beams using
504 neural networks. *Construction and Building Materials*. 2006;20:801-11.
- 505 [43] Jung S, Kim KS. Knowledge-based prediction of shear strength of concrete beams without
506 shear reinforcement. *Engineering Structures*. 2008;30:1515-25.
- 507 [44] Gandomi AH, Yun GJ, Alavi AH. An evolutionary approach for modeling of shear strength
508 of RC deep beams. *Mater Struct*. 2013;46:2109-19.
- 509 [45] Kara IF. Empirical modeling of shear strength of steel fiber reinforced concrete beams by
510 gene expression programming. *Neural Computing and Applications*. 2013;23:823-34.

511 [46] Naik U, Kute S. Span-to-depth ratio effect on shear strength of steel fiber-reinforced high-
512 strength concrete deep beams using ANN model. International Journal of Advanced Structural
513 Engineering. 2013;5:29.

514 [47] Sarveghadi M, Gandomi AH, Bolandi H, Alavi AH. Development of prediction models for
515 shear strength of SFRCB using a machine learning approach. Neural Computing and
516 Applications. 2015.

517 [48] Hossain KMA, Gladson LR, Anwar MS. Modeling shear strength of medium- to ultra-high-
518 strength steel fiber-reinforced concrete beams using artificial neural network. Neural Computing
519 and Applications. 2016.

520 [49] Al-Musawi AA. Determination of shear strength of steel fiber RC beams: application of
521 data-intelligence models. Frontiers of Structural and Civil Engineering. 2018.

522 [50] Flood I. Towards the next generation of artificial neural networks for civil engineering.
523 Advanced Engineering Informatics. 2008;22:4-14.

524 [51] Lantsoght EOL, Van der Veen C, Walraven JC, De Boer A. Database of wide concrete
525 members failing in shear. Magazine of Concrete Research. 2015;67:33-52.

526 [52] Reißer K, Hegger J. Experimental Study on the Shear Capacity of Concrete Slabs. IABSE
527 20112011.

528 [53] Reißer K, Hegger J. Experimentelle Untersuchungen zur mitwirkenden Breite für Querkraft
529 von einfeldrigen Fahrbahnplatten. Beton- und Stahlbetonbau. 2013;108:96-103.

530 [54] Reißer K, Hegger J. Experimentelle Untersuchungen zum Querkrafttragverhalten von
531 auskragenden Fahrbahnplatten unter Radlasten. Beton- und Stahlbetonbau. 2013;108:315-24.

532 [55] Regan PE. Shear Resistance of Concrete Slabs at Concentrated Loads close to Supports.
533 London, United Kingdom: Polytechnic of Central London; 1982. p. 24.

534 [56] Regan PE, Rezai-Jorabi H. Shear Resistance of One-Way Slabs under Concentrated Loads.
535 ACI Structural Journal. 1988;85:150-7.

536 [57] Furuuchi H, Takahashi Y, Ueda T, Kakuta Y. Effective width for shear failure of RC deep
537 slabs. Transactions of the Japan concrete institute. 1998;20:209-16.

538 [58] Sherwood EG, Lubell AS, Bentz EC, Collins MR. One-way shear strength of thick slabs and
539 wide beams. ACI Structural Journal. 2006;103:794-802.

540 [59] Vaz Rodrigues R. Shear Strength of RC bridge deck cantilevers. 6th International PhD
541 Symposium in Civil Engineering. Zurich, Switzerland: Fédération Internationale du Béton; 2006.
542 p. 8 pp.

543 [60] Vaz Rodrigues R, Muttoni A, Olivier O. Large Scale Tests on Bridge Slabs Cantilevers
544 Subjected to Traffic Loads. 2nd international FIB Congress. Naples, Italy: Fédération
545 Internationale du Béton; 2006. p. 10.

546 [61] Jaeger T, Marti P. Reinforced Concrete Slab Shear Prediction Competition: Experiments.
547 Aci Structural Journal. 2009;106:300-8.

548 [62] Jäger T. Querkraftwiderstand und Verformungsvermögen von Stahlbetonplatten. Zurich:
549 ETH Zurich; 2007.

550 [63] Jäger T. Versuche zum Querkraftwiderstand und zum Verformungsvermögen von
551 Stahlbetonplatten. Zurich: ETH Zurich; 2005. p. 362.

552 [64] Graf O. Versuche über die Widerstandsfähigkeit von Eisenbetonplatten unter konzentrierter
553 Last nahe einem Auflager Deutscher Ausschuss für Eisenbeton. 1933;73:10-6.

554 [65] Richart FE. Reinforced Concrete Wall and Column Footings: part 1. ACI Journal
555 Proceedings. 1948;45:97-127.

556 [66] Richart FE. Reinforced Concrete Wall and Column Footings: part 2. ACI Journal
557 Proceedings. 1948;45:237-60.

558 [67] Richart FE, Kluge RW. Tests of reinforced concrete slabs subjected to concentrated loads; a
559 report of an investigation. University of Illinois Engineering Experiment Station Bulletin No
560 314. Urbana: University of Illinois; 1939. p. 86.

561 [68] Serna-Ros P, Fernandez-Prada MA, Miguel-Sosa P, Debb OAR. Influence of stirrup
562 distribution and support width on the shear strength of reinforced concrete wide beams. Magazine
563 of Concrete Research. 2002;54:181-91.

564 [69] Leonhardt F, Walther R. Beiträge zur Behandlung der Schubprobleme in Stahlbetonbau - 2.
565 Fortsetzung des Kapitels II. Versuchsberichte. Beton- und Stahlbetonbau. 1962;57:54-64.

566 [70] Leonhardt F, Walther R. The Stuttgart shear tests, 1961; contributions to the treatment of the
567 problems of shear in reinforced concrete construction. London: Cement and Concrete
568 Association; 1962.

569 [71] Diaz de Cossio R, Moe J, Gould PL, Meason JG. Shear and diagonal tension - Discussion.
570 ACI Journal Proceedings. 1962;59:1323-39.

571 [72] Kani MW, Huggins MW, Wittkopp RR. Kani on Shear in Reinforced Concrete. Toronto:
572 Univ of Toronto, Dept of Civil Engineering; 1979.

573 [73] Rajagopalan KS, Ferguson PM. Exploratory shear tests emphasizing percentage of
574 longitudinal steel. ACI Journal Proceedings. 1968;65:634-8.

575 [74] Aster H, Koch R. Schubtragfähigkeit dicker Stahlbetonplatten. Beton- und Stahlbetonbau.
576 1974;69:266-70.

577 [75] Reineck K-H, Koch R, Schlaich J. Shear Tests on Reinforced concrete beams with axial
578 compression for offshore structures. Institut für Massivbau, Universität Stuttgart 1978.

579 [76] Heger FJ, McGrath TJ. Design method for reinforced concrete pipe and box sections. In:
580 Association TCotACP, editor. Cambridge, Massachusetts; San Francisco, California: Simpson
581 Gumpertz & Heger Inc.; 1980. p. 243.

582 [77] Cullington DW, Daly AF, Hill ME. Assessment of reinforced concrete bridges: Collapse
583 tests on Thurloxton underpass. Bridge Management. 1996;3:667-74.

584 [78] Coin A, Thonier H. Essais sur le cisaillement des dalles en béton armé. Annales du bâtiment
585 et des travaux publics. 2007;7-16.

586 [79] Olonisakin AA, Alexander SDB. Mechanism of shear transfer in a reinforced concrete beam.
587 Canadian journal of civil engineering. 1999;26:810-7.

588 [80] Ekeberg PK, Sjurzen A, Thorenfeldt E. Load-carrying capacity of continuous concrete slabs
589 with concentrated loads (in Norwegian). Nordisk betong. 1982;4:153-6.

590 [81] Rombach GA, Velasco RR. Schnittgrößen auskragender fahrbahnplatten infolge von
591 radlasten nach DIN-fachbericht. Beton- und Stahlbetonbau. 2005;100:376-89.

592 [82] Rombach GA, Latte S. Shear resistance of bridge decks without shear reinforcement.
593 International FIB Symposium 2008. Amsterdam, The Netherlands: Fédération Internationale du
594 Béton; 2008. p. 519-25.

595 [83] Rombach G, Latte S, Steffens R. Querkrafttragfähigkeit von Fahrbahnplatten ohne
596 Querkraftbewehrung. Forschung Straßenbau und Straßenverkehrstechnik. 2009:94.

597 [84] Miller RA, Aktan AE, Shahrooz BM. Destructive testing of decommissioned concrete slab
598 bridge. Journal of Structural Engineering-Asce. 1994;120:2176-98.

599 [85] Fang IK, Tsui CKT, Burns NH, Klingner RE. Load Capacity of Isotropically Reinforced,
600 Cast-in-Place and Precast Panel Bridge Decks. PCI Journal. 1990;35:104-13.

601 [86] Lantsoght EOL. Shear in Reinforced Concrete Slabs under Concentrated Loads Close to
602 Supports: Delft University of Technology; PhD Thesis; 2013.

603 [87] Mohammadyan-Yasouj SE, Marsono AK, Abdullah R, Moghadasi M. Wide Beam Shear
604 Behavior with Diverse Types of Reinforcement. ACI Structural Journal. 2015;112:199-208.

605 [88] van der Veen C, Gijsbers FBJ. Working set factors existing concrete bridges - Memo shear
606 assessment existing bridges. 2011. p. 6.

- 607 [89] Lantsoght EOL, Abambres M. dataset ANN. Zenodo2018.
608 <http://doi.org/10.5281/zenodo.2526405>
- 609 [90] The Mathworks I. Matlab R2017a, User's Guide. Natick, USA2017.
- 610 [91] Abambres M. ANN Software Validation Report. Figshare2018. doi:
611 10.6084/m9.figshare.6962873
- 612 [92] Abambres M, Marcy M, Doz G. Potential of Neural Networks for Structural Damage
613 Localization. ACI Avances en Ciencia e Ingenierias. 2019;11.
- 614 [93] Abambres M, Lantsoght EOL. Neural Network-Based Formula for Shear Capacity
615 Prediction of One-Way Slabs Under Concentrated Loads (preprint). OSF Preprints. 2018.
- 616 [94] Abambres M. W and b arrays. Zenodo2018. <http://doi.org/10.5281/zenodo.2526426>
- 617 [95] CEN. Eurocode 2: Design of Concrete Structures - Part 1-1 General Rules and Rules for
618 Buildings. NEN-EN 1992-1-1:2005. Brussels, Belgium: Comité Européen de Normalisation;
619 2005. p. 229.
- 620 [96] Regan PE. Shear resistance of members without shear reinforcement; proposal for CEB
621 Model Code MC90. London, UK: Polytechnic of Central London; 1987. p. 28.
- 622 [97] ACI Committee 318. Building code requirements for structural concrete (ACI 318-14) and
623 commentary. Farmington Hills, MI: American Concrete Institute; 2014.
- 624 [98] Cope RJ. Flexural Shear Failure of Reinforced-Concrete Slab Bridges. Proceedings of the
625 Institution of Civil Engineers Part 2-Research and Theory. 1985;79:559-83.

626 [99] Cope RJ, Clark LA. Concrete slabs : analysis and design. London: Elsevier Applied Science;
627 1984.

628 [100] Cope RJ, Rao PV. SHEAR FORCES IN EDGE ZONES OF CONCRETE SLABS.
629 Structural Engineer. 1984;62:87-92.

630 [101] Cope RJ, Rao PV, Edwards KR. Shear in skew reinforced concrete slab bridges – analytical
631 and experimental studies – A report to the Department of Transport. Liverpool, UK: University
632 of Liverpool; 1983. p. 219.

633 [102] Lantsoght EOL, de Boer A, van der Veen C. Distribution of peak shear stress in finite
634 element models of reinforced concrete slabs. Engineering Structures. 2017;148:571-83.

635 [103] Wood RH. The reinforcement of slabs in accordance with a pre-determined field of
636 moments. Concrete. 1968;February:69-76.

637 **Acknowledgments**

638 The authors are grateful for the financial support received from Universidad San Francisco de
639 Quito through the 2019 ‘Collaboration Grants’ program.

Conflic of interest

The authors declare no conflict of interest.

Author statement

Section 1, 4, and 8: Abambres M.

Sections 1, 2, 3, 5, 6, 7, and 8: Lantsoght E.